Available online at www.sciencedirect.com
SCIENCE DIRECT®
Journal of Power Sources 138 (2004) 226–231
JOURNAL OF POWER SOURCES
www.elsevier.com/locate/jpowsour

Evaluation on a water-based binder for the graphite anode of Li-ion batteries

S.S. Zhang*, K. Xu, T.R. Jow

U.S. Army Research Laboratory, Adelphi, MD 20783-1197, USA

Received 10 May 2004; accepted 30 May 2004
Available online 30 July 2004

Abstract

We evaluate poly(acrylamide-co-diallyldimethylammonium chloride) (AMAC) as a water-based binder for the graphite anode of Li-ion batteries. It is shown that AMAC has a similar bonding ability as the conventional poly(vinylidene fluoride) (PVDF) binder, and that the graphite electrodes bonded by AMAC and PVDF have nearly the same cyclability. Advantages of AMAC binder include: (1) it assists in forming a more conductive solid electrolyte interface (SEI) on the surface of graphite and (2) organic liquid electrolyte exhibits better penetration on the AMAC-bonded electrode. Impedance analysis shows that formation of the SEI on the surface of graphite includes two stages. The first stage takes place above 0.15 V and the second stage between 0.15 and 0.04 V. The SEI formed in the first stage is relatively resistive, while that formed in the second stage is highly conductive. For the first stage, the presence of AMAC may enhance the conductivity of the SEI. We performed a storage test on the AMAC-bonded graphite by monitoring the change of open-circuit voltage (OCV) of fully lithiated Li/graphite cells and by comparing their capacity change before and after storage. We observed that OCV of the cell increased gradually, and that capacity loss during the storage recovered in the subsequent lithiation process. Therefore, the OCV increase could be considered a self-delithiation process, which does not consume permanently Li^+ ions.

Keywords: Binder; Graphite anode; Solid electrolyte interface; Self-delithiation; Li-ion battery

1. Introduction

Poly(vinylidene fluoride) (PVDF) has been a prefered binder for the graphite anode of Li-ion batteries. However, there is currently a trend to replace the PVDF binder in the anode of Li-ion batteries because of its reactivity with lithium metal and lithiated graphite (Li_xC_6). It has been reported that at elevated temperatures, all fluorinated polymers react with lithium metal and lithiated graphite (Li_xC_6) to form more stable LiF and >C=CF– double bonds, and that the presence of liquid electrolyte increases and accelerates the resulting reactions [1–3]. Furthermore, these reactions are very exothermic, which could cause self-heating thermal runaway. Therefore, safety concerns with Li-ion batteries arise from the use of PVDF in the graphite anode. For the above reasons, much of effort has been undertaken to search for non-fluorinated binders [4–8], most of which are only soluble in organic solvents, such as, silica-based gel [5], aromatic polyimide [6], poly(acrylonitrile-methyl methacrylate) copolymer [7], and hydrocarbon polymer [8]. This means that environmental hazard organic solvents must be adopted for the coating process when using these binders. The preferable content of solids for the slurry coating is 20–30 wt.%. In other words, electrode fabrication needs 70–80 wt.% of organic solvents while most of these solvents evaporate into air during the subsequent drying process. It not only pollutes atmosphere, but also increases the cost of the electrode fabrication due to consumption of expensive organic solvents. Therefore, developing an alternative binder that is applicable to an inexpensive and environmentally friendly solvent is highly desirable.

In an effort to develop rechargeable Li/S batteries [9], we found that water soluble poly(acrylamide-co-diallyldimethylammonium chloride) (AMAC called hereafter), with the chemical structure shown below, has many advantages.

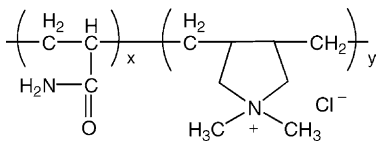

AMAC

* Corresponding author. Tel.: +1-301-394-0981; fax: +1-301-394-0273.
E-mail address: szhang@arl.army.mil (S.S. Zhang).

0378-7753/$ – see front matter © 2004 Elsevier B.V. All rights reserved.
doi:10.1016/j.jpowsour.2004.05.056

It has been found that AMAC binder has a good catalytic effort on the cell reaction of the Li/S battery, and that the liquid electrolyte exhibits an improved penetration on the AMAC-bonded electrode. However, so far AMAC has not been tried in the graphite anode of Li-ion batteries. In this work, therefore, we evaluate AMAC as a water-based binder of the graphite anode by comparing it with conventional PVDF. We studied formation of the SEI in the presence of AMAC by electrochemical impedance spectroscopy (EIS) and evaluated the storage performance of the AMAC-bonded electrode by monitoring change of the OCV of fully lithiated Li/graphite cells.

2. Experimental

Natural graphite powder (distributed by International Technology Exchange Society, Code No. LF-18A) was used as an electrode active material. A 10 wt.% of AMAC solution in water, purchased from Aldrich, was used as the binder and water as the additional solvent. A slurry consisting of 95 wt.% graphite and 5 wt.% AMAC was prepared by ball-milling for 6 h, and then coated onto a copper foil. For comparison, a PVDF-bonded electrode with the same loading and composition also was made by using N-methyl pyrrolidinone solvent. Both slurry coatings were naturally dried in air and cut into small discs with an area of 1.27 cm^2. Before use, the electrodes were further dried at 120 °C under vacuum for 16 h. A solution of 1.0 m $LiPF_6$ dissolved in 3:7 (weight ratio) mixture of ethylene carbonate and ethyl methyl carbonate with a water content of 10–20 ppm was used as the liquid electrolyte. In an argon-filled glove box, BR2335-type Li/graphite button cells were assembled and filled with 150 μL of liquid electrolyte.

A Tenney Environmental Oven Series 942 was used to provide a constant temperature environment for the tests and a Maccor Series 4000 tester was used to perform galvanostatic cycling tests and to record the OCV of the cell. A Solartron SI 1287 Electrochemical Interface and a SI 1260 Impedance/Gain-Phase Analyzer, controlled by CorrWare and Zplot software, were used to record the EIS of the cell. The EIS was potentiostatically measured at the cell's OCV with an ac oscillation of 10 mV amplitude over the frequency range 100 kHz to 0.01 Hz. The stable voltage, at which the EIS was measured, was achieved by cycling galvanostatically the cell at 0.1 mA cm^{-2} to a desired value and then leaving it on open circuit for 10 min. The collected EIS was fitted using ZView software.

3. Results and discussion

3.1. AMAC versus PVDF

AMAC is an ammonium-based cationic copolymer, which has been widely used as an antistatic additive in paper industry. Due to the hydrophilic properties of ammonium and amide components, the polymer is soluble in water and substantially insoluble in most organic solvents. Its aqueous solution has high viscosity and is non-foaming even at high concentrations. These features make it suitable for the slurry coating process. To evaluate AMAC as a binder of the graphite anode, we coated two graphite films with the same loading onto copper foils by using 5 wt.% of AMAC and PVDF, respectively, as the binder. After drying at 120 °C under vacuum for 6 h, the films were performed a "scratch off" test by using a flat knife to scratch graphite coating off the copper substrate. This experiment showed that the graphite anodes bonded with AMAC and PVDF have nearly the same adhesion to the copper substrate. The same conclusion also was made from a "peel-off" test by sticking a 3 M Scotch tape on the graphite coating and then peeling it from the substrate. In addition, we found that AMAC-bonded graphite anode can be calendared freely and folded without surface cracking. The experiments above indicate that, from the standpoint of electrode adhesion, the AMAC-bonded electrode could be strong enough to withstand the normal operation of battery assembly.

Penetration of liquid electrolyte into the graphite anode was evaluated by a means of a visual method. A fixed amount of droplet of propylene carbonate (PC) was dropped onto two graphite anodes with different binder. The PC initially stayed as a droplet on the surface of both graphite anodes and gradually spread out. It is shown that spreading of the PC droplet was slightly faster on the AMAC-bonded graphite than on the PVDF-bonded one. Furthermore, this phenomenon became more obvious when PC was replaced by a 1.0 m $LiBF_4$ PC solution. We consider that the improved penetration of the liquid electrolyte into the AMAC-bonded graphite is likely associated with the interaction between the polar solvent and the cationic polymer. It should be noted that penetration of the liquid electrolyte in Li-ion batteries could be much better than the observation above because the practical electrolyte contains one or more co-solvents with low viscosity and boiling point such as dimethyl carbonate and diethyl carbonate, which are known to increase significantly the penetration of the electrolyte. On the other hand, the feature of AMAC being insoluble in most organic solvents may be helpful for the binder of the graphite anode. Without swelling by the liquid electrolyte, the AMAC-bonded anode is able to retain constant dimensions even at elevated temperatures.

3.2. Reductive stability of AMAC

It is known that organic amides with low molecular weight could be reduced under highly reducting environments when they are dissolved into a solvent or are in a molten state. This fact raises a suspicion about the chemical stability of AMAC as a binder in the graphite anode because of the amide functional groups being present in AMAC molecule. Consequently, we performed a cyclic voltammetry test by using Li

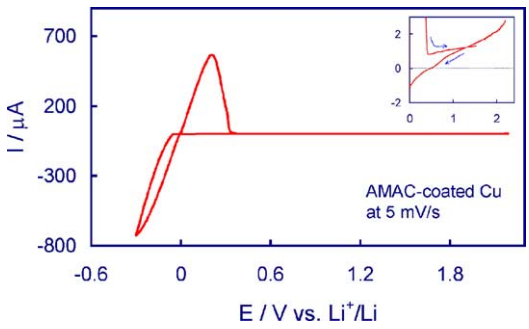

Fig. 1. Cyclic voltammogram of the first cycle of copper wire coated with porous AMAC film, which was recorded at 5 mV s^{-1} in 1.0 m $LiPF_6$ 3:7 EC/EMC electrolyte. Inset is a view with a very small current scale.

foils as the reference and counter electrodes. The working electrode was a freshly scratched copper wire coated with a thin layer of porous AMAC film, in which the pores allow liquid electrolyte to fill in so that ionic conducting pathway between copper and liquid electrolyte can be formed. Fig. 1 shows cyclic voltammogram of the first cycle. Near 0 V versus Li^+/Li, there is a pair of redox current peaks, which is known a characteristic of plating and stripping of lithium. Above the potentials of plating and stripping of lithium, we did not see any other current peaks except for very low leakage currents with a nearly linear *I–E* response (see inset of Fig. 1), which is a characteristic of a double-layer capacitor of the porous electrode. The above results indicate that AMAC is electrochemically stable as a binder in the graphite anode of Li-ion batteries because lithiation and delithiation of graphite take place in a narrow potential range of 0.1–0.4 V versus Li^+/Li. We consider that the excellent stability of AMAC can be attributed to its insolubility in the liquid electrolyte.

3.3. SEI formation with AMAC-bonded graphite

Formation of a stable SEI on the surface of graphite is an essential process for the fabrication of Li-ion batteries, which must be completed in the initial few cycles. Because binder molecules adhere graphite particles and bind them onto the copper substrate, the properties of the binder could affect the formation of the SEI. The effect of binders on reversibility of the initial three cycles of Li/graphite cell is shown in Fig. 2, which was recorded at a very low current density (0.03 mA cm^{-2}). Coulombic efficiency (CE) in the first cycle was relatively low (~70%), however, it increased significantly with the cycle number. It is determined that CE of the initial three cycles were 68.6, 92.6 and 94.4% for the PVDF cell (Fig. 2a), and 70.9, 90.7 and 90.4% for AMAC cell (Fig. 2b). As indicated by the arrows in Fig. 2a and b, irreversible capacities near 0.04 V vanish rapidly with the cycle number. This fact suggests that the irreversible capacities near −0.04 V could be responsible for the formation of the SEI. It is noted that the CE could not approach 100% even in the third cycle. This is because the current density

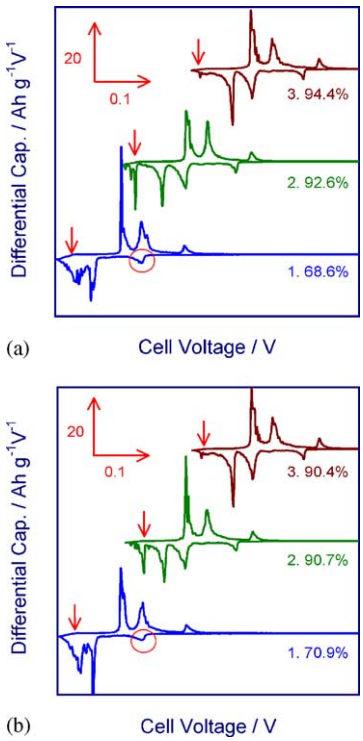

Fig. 2. Plots of differential capacity versus cell voltage for the initial three cycles of Li/graphite cells, which were recorded at 0.03 mA cm^{-2}. Note that a shift has been added to the plots of the second and third cycles for the purpose of graph clarity. (a) PVDF and (b) AMAC.

used for SEI formation was very low. It is known that, during formation, the SEI undergoes two opposite processes: an increased growth and a decreased dissolution. When current density was low, the decreased dissolution might become predominant so that the cycling suffered a low CE. This speculation has been confirmed by the following fact. When the current density was increased to 0.1 mA cm^{-2} (~*C*/10), CE of the initial three cycles accordingly rose to 84.1, 97.3 and 98.3% for the PVDF cell and to 80.3, 97.0 and 97.9% for the AMAC cell.

The EIS technique has been an effective tool for studying of the SEI formation. Before discussing the SEI formation, we should clarify the relationship of EIS and cell voltage (i.e., so-called "state of lithiation"). Fig. 3 displays EIS of the Li/graphite at various voltages, which were recorded during the delithiation process of the tenth cycle. It is clear that the EIS contains two overlapped semicircles and it varies significantly with cell voltage. As discussed elsewhere [10–12], each semicircle can be fitted by a parallel equivalent circuit consisting of a resistance and a capacitor. In general, the semicode at high frequency reflects the impedance (Z_{SEI}) of the SEI and the other semicode at low frequency regions reflects the impedance (Z_{ct}) of the charge-transfer process. The straight sloping line at low frequency relates to impedance (Z_d) of a diffusion process of Li^+ ion in the electrolyte-electrode interface. The Combination of Z_{ct} and Z_d is called Faradic impedance, which reflects the kinetics

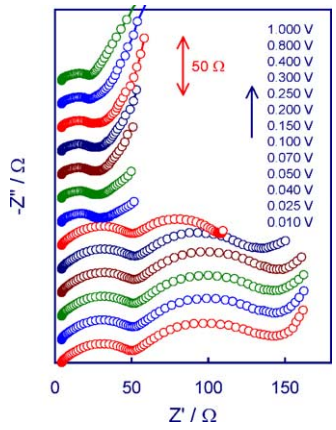

Fig. 3. EIS of the Li/graphite cell with AMAC binder at various voltages, which were recorded at 30 °C during delithiation process of the 10th cycle.

of the cell reaction. The Z_{SEI} consists of a parallel combination of the SEI resistance (R_{SEI}) and its related capacitance (C_{SEI}). The values of R_{SEI} are fitted using ZWiew software and are plotted as a function of the cell voltage in Fig. 4. Observing R_{SEI} of the 10th cycle at which the SEI is assumed to be fully formed, one finds that the R_{SEI} is increased significantly at ~0.07 V in the lithiation process and decreased reversibly to the original level at ~0.1 V in the delithiation process. More interestingly, such changes of the R_{SEI} versus cell voltage correspond to the peaks of differential capacities very well. The observations above are independent of the binder and electrolyte formulation. Similar phenomena

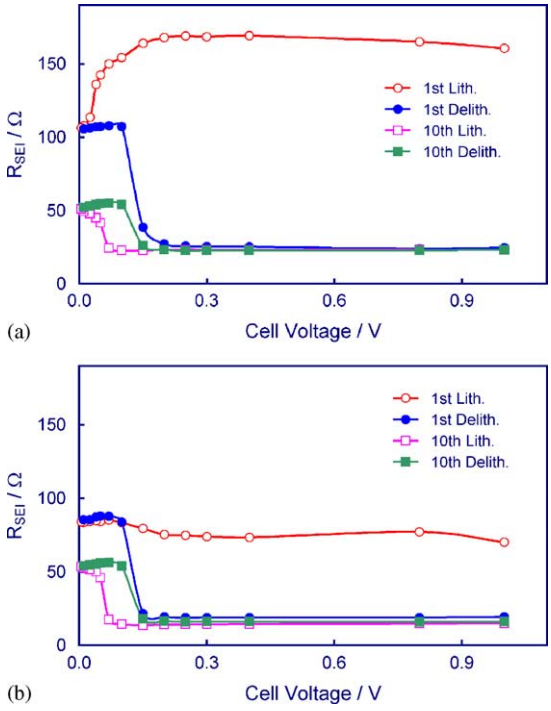

Fig. 4. Change of the SEI resistance (R_{SEI}) with cell voltage of the Li/graphite cell during lithiation and delthiation in the first and tenth cycles. (a) PVDF and (b) AMAC.

also were observed from other sources by independent researchers [10–12]. It is believed that such changes relate to an expansion and contraction of the graphite volume, caused by the lithiation and delithiation processes.

Significant difference in the R_{SEI}–E correlation between PVDF and AMAC is observed from the first lithiation process (as shown by open circles in Fig. 4a and b). Overall, the cell with AMAC binder has much lower R_{SEI} than the one with PVDF binder. Although being narrowed, such a trend still remained after the SEI was fully formed. For example, the R_{SEI} above 0.2 V constantly remained at 16 Ω for AMAC cell and at 23 Ω for PVDF cell. The above facts reveal that the presence of AMAC favors increasing conductivity of the SEI. For the same reason as described previously [10], the formation of the SEI during the first lithiation process can be divided into two voltage regions. The most positive voltage peak of the differential capacities, as marked by a small circle in Fig. 2a and b, serves as a border of these two voltage regions.[1] In the higher voltage regions where the lithiation is assumed not to take place, a resistive SEI is formed so that the R_{SEI} increases slowly with the decrease of cell voltage. In the lower voltage regions where the lithiation is in progress, a highly conductive SEI is formed so that the R_{SEI} decreases significantly with the decrease of cell voltage. For both PVDF and AMAC, the most positive voltage peak of the differential capacity is around 0.15 V (as indicated by a small circle in Fig. 2a and b), above which the R_{SEI} increases slowly with the decrease of the cell voltage. Below 0.15 V, the R_{SEI}–E correlation becomes rather complicated, which reflects a combined effect of two opposite changes: (1) formation of the highly conductive SEI, which results in a decrease in the R_{SEI}, and (2) volume expansion of graphite, which leads to an increase in the R_{SEI}. In the PVDF cell, the first effect is predominant so that its R_{SEI} decreases rapidly with the decrease of cell voltage (Fig. 4a). In AMAC cell, two opposite changes appear to offset each other so that R_{SEI} only presents a small fluctuation with the decrease of cell voltage (Fig. 4b).

3.4. Storage and cycling performance of AMAC-bonded graphite

Storage and cycling tests were performed to evaluate the chemical stability of AMAC with respect to the highly reductive lithiated graphite (Li_xC_6). Response of the OCV to storage time at 60 °C is plotted in Fig. 5, in which a voltage-capacity curve for a galvanostatic delithiation process is also plotted for the purpose of comparison. It is seen that the OCV rises slowly with storage time through three voltage plateaus. This observation is in good agreement with

[1] The most positive voltage peak of the differential capacity in the first lithiation process may be shifted by electric polarization, which is associated with the resistance of the initially formed SEI and is affected by many factors such as the type of graphite and electrolyte, formulation and loading of the graphite electrode.

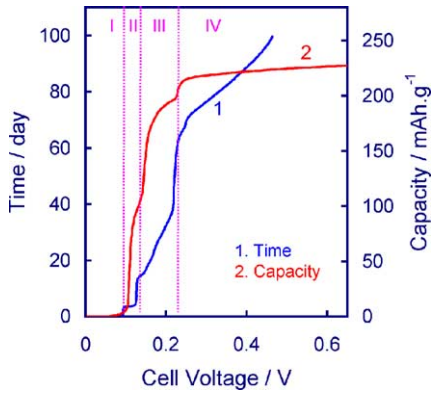

Fig. 5. Voltage curves of a self-delithiation process at 60 °C and of a galvanostatic delithiation process at 0.03 mA cm^{-2} for fully lithiated Li/graphite cells.

the voltage-capacity curve of a normal delithiation process, in which the voltage plateaus are known to reflect three continuous phase transitions (i.e., I → II → III → IV, as shown in Fig. 5). To find correlation between the OCV increase and delithiation, we plot differential time and differential capacity for the storage and galvanostatic delithiation process, respectively, versus cell voltage in Fig. 6. Obviously, both differential time and differential capacity present three peaks with a change in the cell voltage. Taking the IR drop suffered in the galvanostatic delithiation process into account, one may find that the voltage regions of each plateau, as marked by numbers in Fig. 6, in the storage and delithiation processes are consistent with each other. In addition, we found that capacity loss during the storage is recoverable in the subsequent lithiation process. Therefore, the OCV increase observed in Fig. 5 can be attributed to a self-delithiation process, which can be expressed by the reaction [13–15]:

$$Li_xC_6 \rightarrow Li_{x-\delta}C_6 + \delta Li^+ + \delta e$$

The mechanism of the self-delithiation is unclear. Probably, it is associated with a local redox process on the graphite

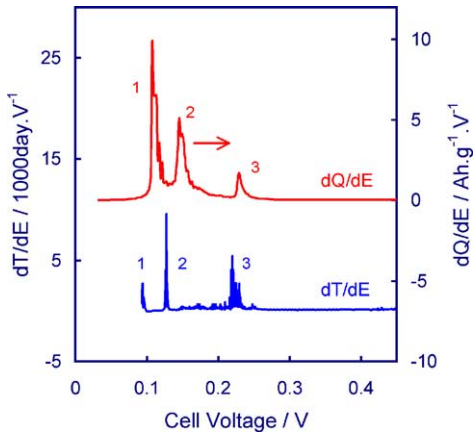

Fig. 6. Plots of differential time and differential capacity versus cell voltage for the self-delithiation and galvanostatic delithiation process, respectively, of fully lithiated Li/graphite cells.

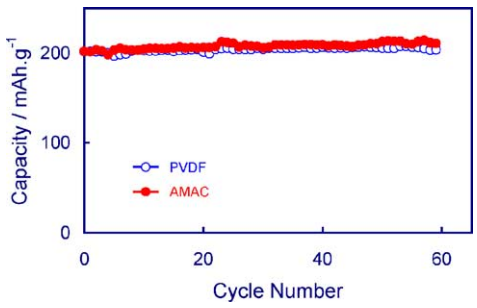

Fig. 7. Delithiation capacities of Li/graphite cells as a function of the cycle number, which were measured by cycling galvanostatically the cells at 0.5 mA cm^{-2} between 0.002 and 1.0 V. Before cycling test, both cells were stored at 60 °C for 100 days.

electrode, which involves a chemical reduction of the electrolyte solvents. A supporting evidence is that the rate of the self-delithiation was significantly accelerated when graphite was flooded in an extra liquid electrolyte [14].

Delithiation capacities of the Li/graphite cell with different binders are plotted as a function of the cycle number in Fig. 7, which shows that the cells with PVDF and AMAC have nearly the same cycling performance. This observation verifies that AMAC might not have an adverse impact on the cycling of lithiation and delithiation of graphite, and that AMAC could be electrochemically stable as a binder of the graphite anode in Li-ion batteries. It should be noted that the delithiation capacities obtained in this work are relatively low in comparison to the theoretical capacity of graphite, which is due to different cycling conditions. As we know, many capacities of graphite are present near the low cut-off voltage. Full capacity can be achieved only when an additional taper lithiation (i.e., lithiation under constant voltage) is added. In this work, the taper lithiation was not applied.

4. Conclusions

Based on the results of this work, we conclude that AMAC is a good binder for the graphite anode of Li-ion batteries. From the standpoint of graphite adhesion to the copper (used as the current collector of the anode), AMAC has a similar binding ability as the conventional PVDF. It appears that AMAC has no adverse impact on the electrochemical properties of graphite, with the following advantages: (1) it uses environmentally friendly water as the processing solvent, (2) graphite anode bonded with it has better wettability and does not swell in organic liquid electrolyte and (3) its presence favors increasing conductivity of the SEI on the surface of graphite.

References

[1] A. Du Pasquier, F. Disma, T. Bowmer, A.S. Gozdz, G. Amatucci, J.M. Tarascon, J. Electrochem. Soc. 145 (1988) 472.

[2] H. Maleki, G. Deng, A. Anani, J. Howard, J. Electrochem. Soc. 146 (1999) 3224.
[3] H. Maleki, G. Deng, I. Kerzhner-Haller, A. Anani, J.N. Howard, J. Electrochem. Soc. 147 (2000) 4470.
[4] M. Gaberscek, M. Bele, J. Drofenik, R. Dominko, S. Pejovnik, Electrochem. Solid-State Lett. 3 (2000) 171.
[5] G. Oskam, P.C. Searson, T.R. Jow, Electrochem. Solid-State Lett. 2 (1999) 610.
[6] N. Ohta, T. Sogabe, K. Kuroda, Carbon 39 (2001) 1434.
[7] S.S. Zhang, T.R. Jow, J. Power Sources 109 (2002) 422.
[8] M.W. Verbrugge, B.J. Koch, J. Electrochem. Soc. 150 (2003) A374.
[9] S.S Zhang, S. Cheng, U.S. Patent 6,110,619, 2000.
[10] S.S. Zhang, M.S. Ding, K. Xu, J. Allen, T.R. Jow, Electrochem. Solid-State Lett. 4 (2001) A206.
[11] R. Yazami, A. Martinent, Y. Reynier, B. Fultz, in: Proceedings of 204th ECS Meeting Abstracts, Orlando, FL, 12–17 October 2003, p. 310.
[12] T. Piao, D.M. Zhou, H. Tsukamoto, in: Proceedings of 204th ECS Meeting Abstracts, Orlando, FL, 12–17 October 2003, p. 352.
[13] A.M. Andersson, K. Edstrom, J. Electrochem. Soc. 148 (2001) A1100.
[14] C. Wang, X.W. Zhang, A.J. Appleby, X. Chen, F.E. Little, J. Power Sources 112 (2002) 98.
[15] S.S. Zhang, K. Xu, T.R. Jow, J. Power Sources 113 (2003) 166.